Int. J. Multiphase Flow, Vol. 2, pp. 435-451. Pergamon/Elsevier, 1976. Printed in Great Britain.

FLOW OF TWO LIQUIDS IN SLOPING TUBES: AN ANALOGUE OF HIGH PRESSURE STEAM AND WATER

G. C. GARDNER and J. KUBIE
Central Electricity Research Laboratories, Leatherhead, Surrey, England

(*Received* 15 *February* 1975)

Abstract—A two-liquid system provides a better analogue for visualization purposes of high pressure boiler systems, where the density ratio is typically 4:1, than air and water at atmospheric pressure. A study is presented of the flow of isoamyl alcohol and water in sloping tubes and a stratified ribbon of alcohol is found, which is not seen with air and water, and this accounts for some corrosion failures in boilers. A critical condition is also encountered when the ribbon starts to be broken into drops and this quantitatively explains the occurrence of a minimum in the curve of burnout heat flux vs water velocity in steam–water systems from 11 to 18 MN/m^2.

1. INTRODUCTION

The impetus for the present work was the failure by corrosion of boiler tubes sloping at 22° to the horizontal. The tubes of 30 mm bore were heated from above and the water within was at 17 MN/m^2 and at zero or near zero quality. Examination of the failed tubes showed a strip of discoloured and corroded internal surface about 10 mm wide at the crown of the cross section and left the impression that there had been a continuous ribbon of separated steam, which permitted the concentration of salts to levels sufficient to cause corrosion. However, the only visual observations available were of an analogue system with air and water at atmospheric pressure and they showed air to be gathered into bubbles which are known (Gardner & Adebiyi 1974) to be separated from the tube wall by a thin liquid film. The bubbles, even though of substantial size, would not be sufficiently large for the film to drain and evaporate to dryness. It was therefore argued that the large density of the steam at 17 MN/m^2 was an important factor and that the frictional drag of the steam with the tube wall would then make it travel at a speed comparable to and even slower than the water. In consequence, a stable stratified "ribbon" flow might be established. On the other hand, frictional effects would be negligible with air at atmospheric pressure and, due to buoyancy, the air would tend to travel much faster than the water. Ribbon flow might be unstable and the bubbles, with much greater form drag, would be formed.

The work to be described was initially aimed at testing the hypothesis stated above but, as will be shown, additional interesting conclusions were achieved. The analogue system chosen for visual observation was isoamyl alcohol saturated with water as the light phase and water saturated with the alcohol as the heavy phase. The principal reasons for this choice were, firstly, that it was believed that slight solubility of the phases in each other would avoid hysteresis effects when one phase displaced the other from part of the tube wall, secondly, that the alcohol could be used with many plastic materials and so simplify rig construction and, lastly, that the alcohol was available pure and in bulk. There was the additional advantages that the interfacial tension was 4.86×10^{-3} J/m^2, which compares very favourably with the value of 3.43×10^{-3} J/m^2 for water at 17 MN/m^2. The density ratio of the phases was 1.2:1, which is substantially different from but very much closer to the value of 4.7:1 for the 17 MN/m^2 steam–water system than about 800:1 for air and water. The difference of the density ratio between the analogue and prototype system is unavoidable in a simple analogue and was accepted because it was expected that a suitable model velocity could be chosen on the basis of a Froude number, which included the phase densities. The agreement between experiment and theory, discussed later, substantiates this view. The difference between model and prototype that was accepted more reluctantly was that the viscosity of the water was much smaller than that of the alcohol. The viscosity ratio was 0.2:1

compared to 2.5:1 for water and steam at 17 MN/m^2. This difference can be substantially removed in future work by using n-butyl acetate, when the viscosity ratio will be 1.5:1, but rig construction will then have to avoid most plastics.

Visual observations were a major part of the experimental program but measurements were also made of the difference between the average phase velocities. It will be seen that the occurrence of ribbon flow was verified and the magnitude of the phase velocity difference is theoretically explained. In addition, a critical condition is defined when the ribbon begins to be broken up into small drops and this is also the subject of a theoretical treatment. Observations and measurements were made for a wide range tube inclinations.

Although emphasis has been laid on the analogy between the present observations and high pressure steam-water flow, the results can, of course, be accepted simply as a study of a liquid–liquid system and may prove valuable in that sense. The only comparable work presented in the literature is by Russell *et al.* (1959) for oil and water in a horizontal pipe. The density ratio was also 1.2:1 but the viscosity ratio was 0.055:1. Stratification was found, similar to that to be described later, but the smallest volumetric fraction of oil was 0.21, whereas the present work concentrated upon much lower values.

2. APPARATUS AND EXPERIMENTS

The apparatus is shown diagrammatically in figure 1. The test section was a 0.6 m long, 32 mm bore glass tube set at each end into plastic ball valves, which provided unobstructed passage to the fluids without change of cross section. Water was introduced axially into a 1 m long calming section of glass tube set before the test section and alcohol was introduced gently through five 10 mm glass tubes at the beginning and in the top of the calming section, because the boiler tubes of interest were heated from the top.

A by-pass tee with a plastic ball valve was provided in the bottom of the calming section just before the test section. All three valves of the test section and the tee were linked by a bar which could be rapidly moved so as to isolate the test section and open the by-pass simultaneously, thus trapping the fluids flowing through the test section at a particular time. The alcohol and any water that came with it could then be drained through two 5 mm bore drains provided in the lower surface of the test section and the alcohol volume measured. It was found that up to 2 cm^3 of alcohol, depending upon the slope of the test section, was retained by the test section upon drainage and this quantity was added to the drained volume. The value of the correction was determined by injecting a known volume of alcohol through one of the drains and measuring the volume recovered by drainage. All this information, together with the total volume of the test section, was used to calculate the volumetric fractional hold-up of alcohol.

The test section discharged into a 32 mm bore tube which curved gently, with a radius of curvature of about 0.3 m, to a vertical run up to a circulating tank. The alcohol and water separated in this tank and different suction lines took them to their respective circulating pumps, after which the flow rates were measured by rotameters. Make-up water to the circulating tank

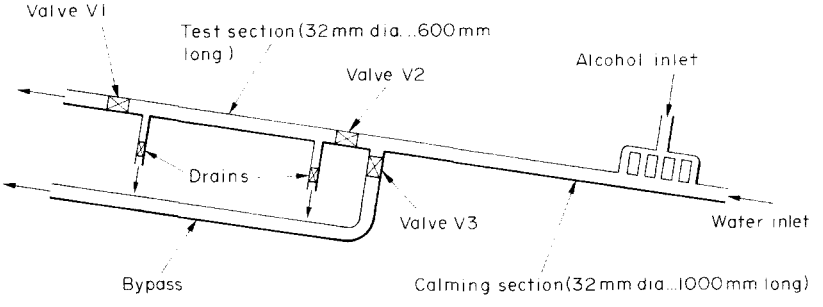

Figure 1. Diagram of the experimental apparatus.

was taken from the town's water supply and filtered through a glass filter to remove silica and other solid matter which otherwise would have fouled the interfaces between alcohol and water. Even with this precaution, it was found that scum formed at the interfaces after a long period of running. The fluids were then replaced but it was never found that the quantitative measurements had been affected by the scum.

The viscosities of the fluids were measured with an Ostwald viscometer and the interfacial tension was measured by the drop weight method.

A run consisted of setting the required alcohol and water flow-rates, making notes of the appearance of the flow and then isolating the test section and measuring the trapped alcohol volume. Separate runs were made to take photographs.

Runs were made over the widest range of flowrates possible with the equipment and as reported later. The tube slope was set at 0°, 16°, 22°, 30°, 45°, 60° and 88° to the horizontal. 88° was chosen rather than 90° since, in the latter case, the equilibrium condition must be one in which the alcohol is dispersed all round the perimeter of the tube or across the cross-section and the intention was to determine if a slight angle to the vertical could give a strong bias to the distribution.

3. EXPERIMENTAL RESULTS

The most detailed experiments were carried out with the tube sloping at 16° to the horizontal and figures 2 and 3 are of photographs taken from above and from the side respectively. V_{LS} and V_{HS} are the superficial velocities of the light and heavy phases respectively. The top four views in figure 2 are for the very small superficial alcohol velocity of 1.6 cm/s and for a superficial water velocity increasing from zero to about 80 cm/s. At zero water velocity there is a well-defined alcohol ribbon with some interfacial disturbances. At a superficial water velocity of 15.7 and 47 cm/s the ribbon remains well-defined but is narrower and more quiescent. The quiescence is most strikingly illustrated in the side views of figure 3, where the superficial alcohol

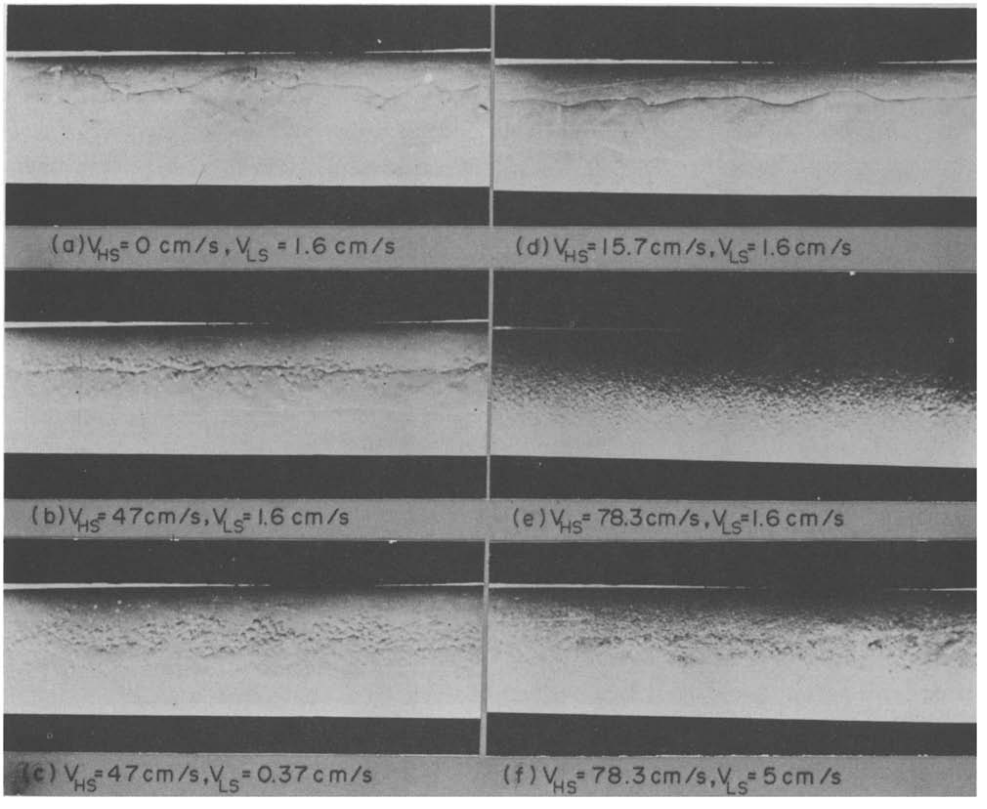

Figure 2. Plan views of alcohol–water flow in a 32 mm tube sloping at 16° to horizontal.

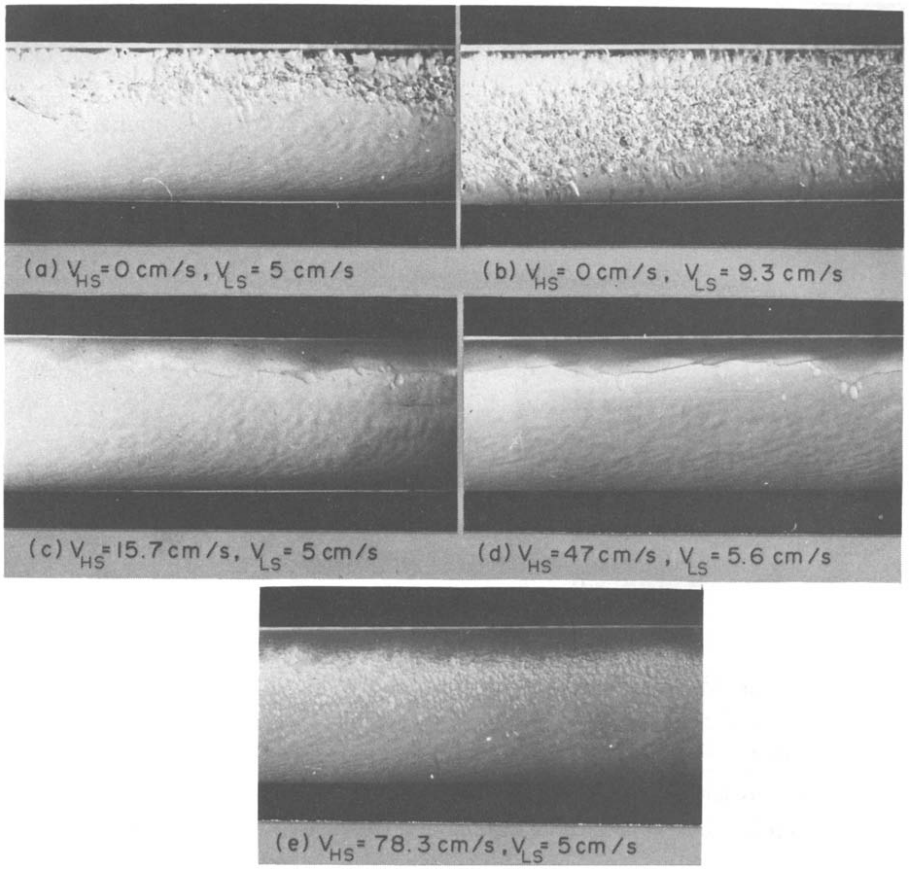

Figure 3. Side views of alcohol–water flow in a 32 mm tube sloping at 16° to horizontal.

velocity is 5 cm/s in order to obtain a sufficiently deep ribbon for observation. There is a very marked change in the interfacial appearance in figure 3 as the superficial water velocity is increased from zero to 15.7 cm/s.

Returning to figure 2, it is observed that small alcohol drops have appeared when the alcohol and water superficial velocities are 1.6 and 47 cm/s respectively. However, these drops are not a dominant feature, as is clear from the corresponding side view for the same water flow in figure 3. A further view in figure 2 for the same water flow but with a much smaller superficial alcohol velocity of 0.37 cm/s shows that a ribbon still remains, with the implication that the drops are much less than 1% of the total flow. At alcohol and water superficial velocities of 1.6 and 78.3 cm/s, on the other hand, the alcohol drops are numerous and, if the alcohol velocity is then increased to 5 cm/s, a ribbon becomes apparent though, again, this is much more obvious in the side view of figure 3, where a clear alcohol layer is seen above a substantial droplet raft.

The last point to note from figure 3, before turning to the associated quantitative measurements, is the large interfacial waves in the two views for zero water velocity. The amplitude of the waves increases as the alcohol depth and flowrate increases.

The influence of all the qualitative features noted above can be seen reflected in the graphs of slip or phase velocity difference—average alcohol velocity less the average water velocity—vs fractional alcohol area shown in figure 4. Each curve is for a constant superficial water velocity, so that the abscissa indicates an increase in superficial alcohol velocity. The average velocity of a phase was calculated in the usual manner by first dividing the volumetric flowrate by the tube's cross-sectional area to obtain the superficial velocity and dividing the result by the fraction of the test section volume occupied by the phase, as found by the drainage procedure detailed in the last section.

The curves in figure 4 for superficial water velocities up to 31.3 cm/s exhibit an upward

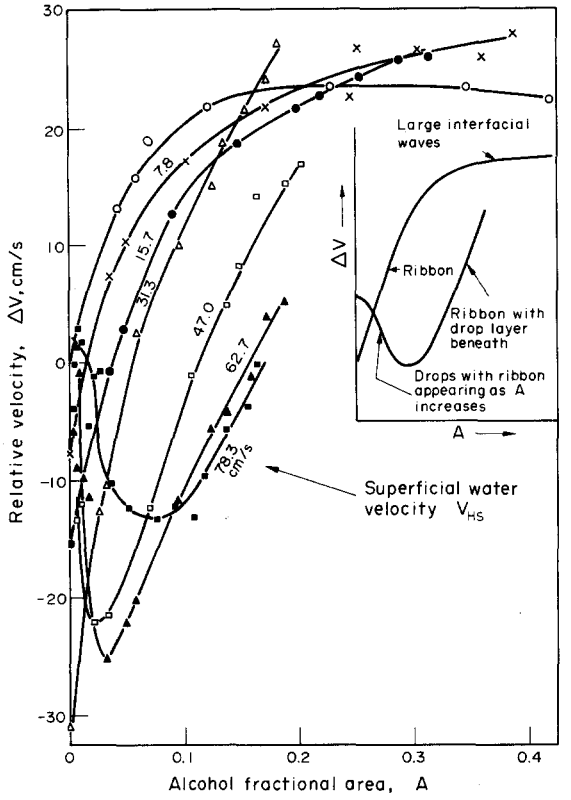

Figure 4. Relative velocity for tube at 16° to horizontal. Inset shows types of flow.

sloping and almost linear section from negative to positive relative velocity, as the alcohol fractional area increases from zero. This section corresponds to pure ribbon flow and it is clear that, when the alcohol flowrate is small, there is sufficient frictional drag for the average alcohol velocity to be less than that of the water. Alcohol drops were observed when the superficial water velocity increased to 47 cm/s and these drops would be expected to travel at approximately the same velocity as the water. Figure 4 shows that curves for velocities of 47 cm/s or more start near zero relative velocity, (in agreement with expectation) rapidly fall to a minimum negative value before rising along a line indicative of the presence of ribbon flow. Therefore, although drops dominate at very small alcohol fractional areas, the influence of the ribbon rapidly becomes apparent, leading at first to negative relative velocity.

The last point to note in figure 4 is that the relative velocity reaches a maximum and level value of about 25 cm/s, at least for the smaller superficial water velocities and larger alcohol fractional areas. The achievement of this maximum corresponds to the appearance of large interfacial waves, which presumably offer substantial form drag.

The visual observations for the horizontal tube were similar to those noted above but the depth of the alcohol layer was larger for the same flow rates. Figure 5 shows that the relative velocity was negative for the range of experiments carried out, because the buoyancy driving force was absent.

Strongly stratified flow occurred at tube angles to the horizontal of up to at least 60°. The photographs of figure 6 show stratification at 45°. They also show drop swarming for low alcohol flowrates and tube slopes of 30° or greater. The ribbon then formed less readily and alcohol drops passed along the upper tube surface in more or less discrete swarms. Sometimes a large drop with the characteristic bullet shape, would be present in the swarm. As a result of this tendency to drop flow and because of the increased buoyancy force, relative velocity is always positive and a fairly weak function of alcohol fractional area for superficial water velocities of 31.3 cm/s and less in figures 8 and 9 for tube slopes of 45° and 60°, respectively. The curve shape characteristic

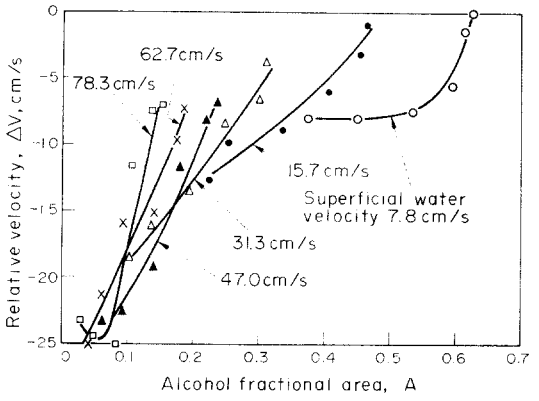

Figure 5. Relative velocity for horizontal tube.

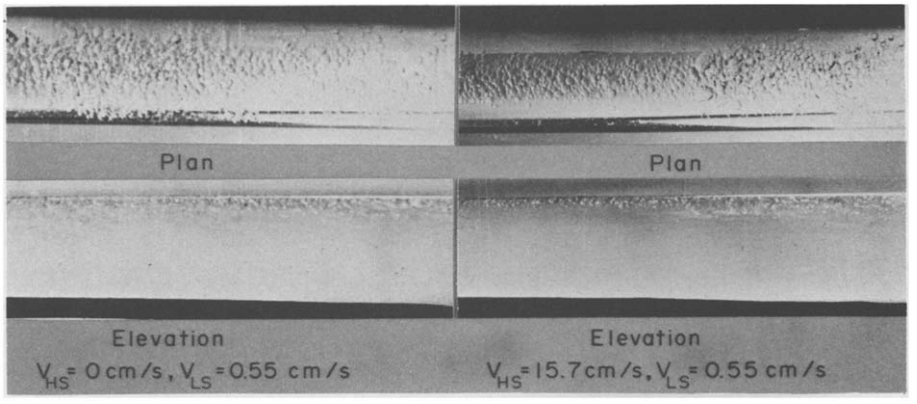

Figure 6. Plan and side views of alcohol–water flow in a 32 mm tube sloping at 45° to horizontal.

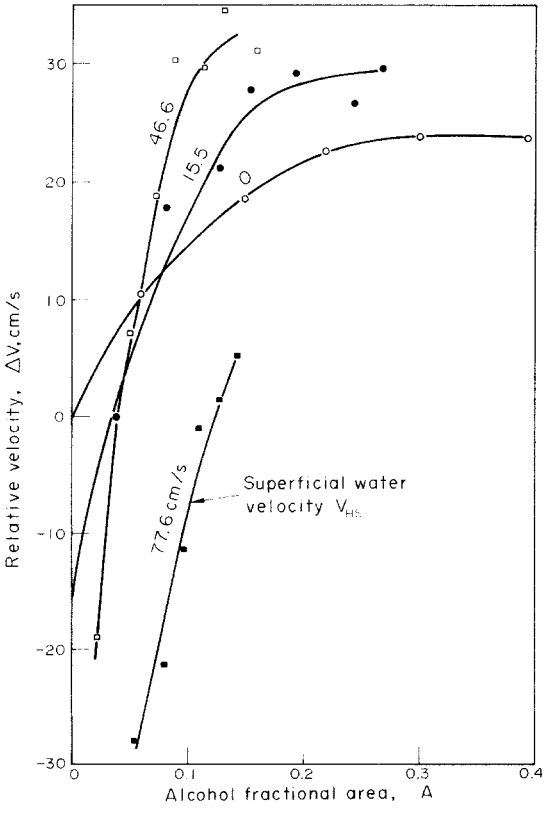

Figure 7. Relative velocity for tube at 30° to horizontal.

or ribbon flow only appears for superficial water velocities of 47 cm/s and more, when it was observed visually that drops tended to be smeared against the tube wall. It is also noted from figures 8 and 9 that the curves for these higher water velocities pass through the band of the less strongly sloping curves for lower velocities and continue upwards with little noticable tendency to level off. The visual observation corresponding to this difference was that there was a substantial raft of drops between the water and the alcohol layers and perhaps this raft damped the large interfacial waves, which were noted previously in figure 3.

With the tube at 88° drop flow was observed under all experimental circumstances and the drop size decreased, in general, with velocity. An interesting point, however, was that the alcohol injected at the wall on one side of the tube (figure 1) tended to remain against the wall for larger

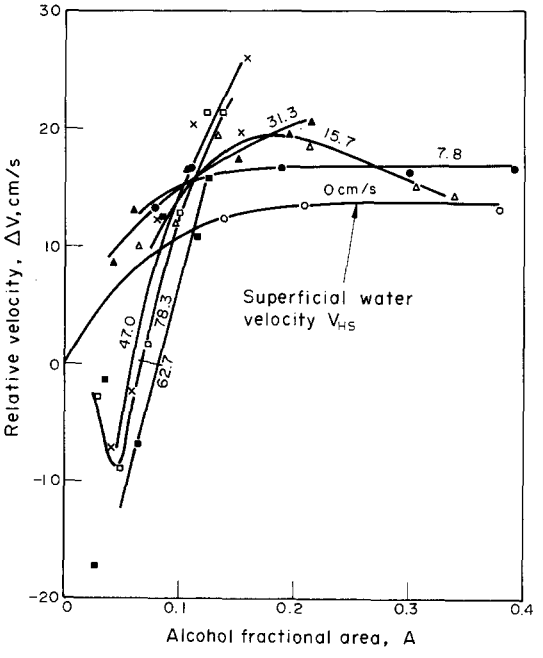

Figure 8. Relative velocity for tube at 45° to horizontal.

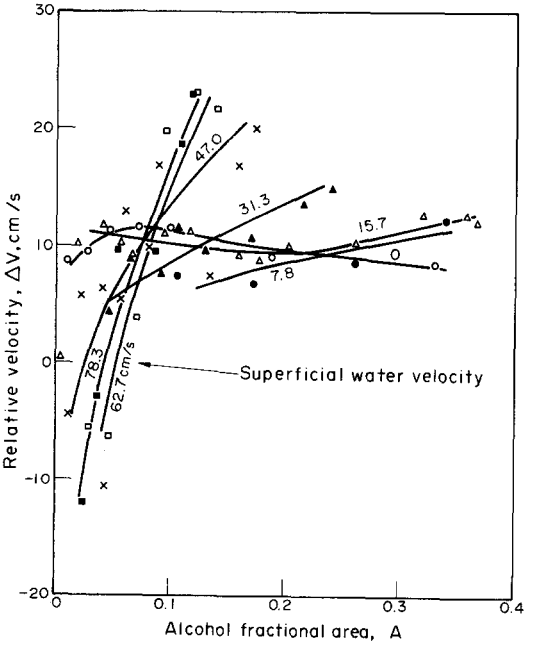

Figure 9. Relative velocity for tube at 60° to horizontal.

distances as the water flowrate was increased. The visual observations left the impression that a substantial ribbon might well exist in a steam–water system in a vertical tube when steam was being preferentially generated on one side of the tube.

4. THEORETICAL TREATMENTS

Two conditions have been found that can conveniently be the subject of a theoretical treatment. The first concerns the condition for the onset of the breakdown of the alcohol ribbon into drops. The second is the operating conditions necessary to give zero slip with ribbon flow as well as the slope of the curve for slip versus the alcohol fractional area at the point of zero slip.

4.1 *Breakdown of the alcohol ribbon into drops*

Gardner & Crow (1973) showed theoretically and experimentally that the critical condition for the entrainment of drops from a horizontal two-phase interface is

$$\frac{\rho_H u^2}{(\Delta\rho g\sigma)^{1/2}} = 3.3, \qquad [1]$$

where ρ_H is the density of the lower phase, $\Delta\rho$ is the density difference between the phases, g is the acceleration due to gravity, σ is the surface tension and u the local velocity of the lower phase normal to the interface. The theory visualized a jet or packet of the lower fluid hitting and distorting the interface. The distortion is resisted both by surface tension and by gravity but, if it exceeds a certain value, the surface is broken and drops of the upper phase are entrained in the lower phase.

In the present case, the lower phase is travelling parallel to the upper phase in a turbulent fashion. Eddies approach the surface with an average velocity of $(f/2)^{1/2}U$ (Hinze 1959), where f is the friction factor and U is the velocity parallel to the surface. Therefore we obtain from [1]

$$\frac{\rho_H f K^2 U_C^2}{(\Delta\rho g\sigma\cos\alpha)^{1/2}} = 6.6, \qquad [2]$$

α is the angle of inclination of the tube to the horizontal and $\cos\alpha$ is introduced to give the appropriate component of the gravitational field normal to the interface. U_C is the critical value of U and the empirical constant K is introduced because eddies with velocities higher than the average value must be expected. Now the value of the Fanning friction factor for a smooth pipe at velocities at or near those at which drops were seen to appear is 0.0065. Further, the critical velocity for $\alpha = 16°$ was found to be between 47 cm/s and 78 cm/s. At the lower velocity drops, were just obvious while at the upper velocity the alcohol ribbon was completely broken up for small alcohol flowrates. Substitution of this data with the appropriate physical properties into [2] gives $K = 3.6$ and 2.16 for the two velocities, respectively. K should be larger than but near unity for the hypothesis to be credible and it clearly satisfies this criterion. Therefore the description of the alcohol ribbon breakdown into drops in the fashion observed here can reasonably be expected to occur in the high pressure boiler, if velocities are scaled according to [2].

There are some results from a high pressure boiling water rig that reinforces this view. It was found by Chojnowski *et al.* (1974) that, if the steam quality is constant, the burnout heat flux for a tube at 22° to the horizontal passes through a minimum with respect to water velocity. This can be interpreted by the observations made in the present study. At low water velocities the steam layer would be disturbed but would become more quiescent and stable as the velocity increased. Therefore the burnout heat flux would be expected to decrease with water velocity but, eventually, the steam layer would be disrupted and form bubbles, so that the burnout heat flux would start to increase. Thus one associates the minimum in the burnout heat flux curve with the

onset of entrainment of steam by the water. The water velocity corresponding to the minimum was 222, 196, 174 and 156 cm/s at 11, 14, 16.5 and 18 MN/m^2, respectively. The Fanning friction factor for all these cases, according to the Moody chart, was 0.0033. Insertion of this data and the appropriate physical properties into [2] gives $K = 2.15$, 2.21, 2.14 and 2.18 for the above pressures, respectively. Therefore [2] predicts the minimum with K equal to the average value of 2.17 and, since this value has been shown above to be equivalent to a superficial water velocity of 78 cm/s in the alcohol–water experiments, the minimum occurs with a condition equivalent to that shown in the photograph of figure 2 for that flowrate.

4.2 *Ribbon flow in the vicinity of zero relative velocity*

It was shown in section 3 that a steadily rising curve of relative velocity vs alcohol fractional area was indicative of ribbon flow, though there might still be a substantial drop raft between the alcohol ribbon and the water. Here we make the assumption that all the alcohol is present as a ribbon with a flat interface that subtends an angle of 2θ to the axis of the tube and estimate the conditions required for zero relative velocity, as well as the slope of the curve at zero relative velocity. Comparison of these estimates with experiments provides two substantially independent checks of the validity of the model.

The tube makes an angle α to the horizontal and the following momentum equations can be written for the light (subscript L) and heavy (subscript H) phases, respectively.

$$-\Delta p A_L + g\rho_L A_L \Delta z \sin\alpha + \tau_{wL} P_L \Delta z + \tau_i P_i \Delta z = 0, \quad [3]$$

$$-\Delta p A_H + g\rho_H A_H \Delta z \sin\alpha + \tau_{wH} P_H \Delta z - \tau_i P_i \Delta z = 0 \quad [4]$$

where Δp is the pressure drop over the tube length Δz, ρ is the density, τ_w is wall shear stress, A_L and A_H are tube cross sectional areas occuped and P_L and P_H perimeters of the tube wetted by the light and the heavy phase respectively, τ_i is the interfacial shear, P_i is the interfacial perimeter and g is acceleration due to gravity.

Eliminating the pressure drop between [3] and [4], introducing the wall friction factor f and using the following dimensionless variables

$$A = A_L/\pi R^2 \quad [5]$$

$$P = P_L/2\pi R \quad [6]$$

$$s = P_i/P_L \quad [7]$$

where R is the tube radius, we finally obtain the following equation

$$1 = \frac{f_L \rho_L V_L^2}{gR\Delta\rho \sin\alpha}\frac{P}{A} - \frac{f_H \rho_H V_H^2}{gR\Delta\rho \sin\alpha}\frac{1-P}{1-A} + \frac{2\tau_i}{gR\Delta\rho \sin\alpha}\frac{sP}{A(1-A)} \quad [8]$$

V_L and V_H are the mean velocities of the light and heavy phases.

It can be shown that the flow of the heavy phase is turbulent for the chosen experimental velocities. Hence it is assumed that f_H is approximately constant. On the other hand the flow of the light phase, though sometimes turbulent, is usually laminar and both flow regimes of the light phase must be considered. When the light phase is turbulent, its friction factor will also be assumed constant and, for present experimental conditions, the turbulent Fanning friction factors are obtained from Moody charts as $f_H = 0.0065$ and $f_L = 0.0095$. It is shown in appendix 1 that the friction factor for the laminar flow of the light phase can be calculated from the following expression

$$f_L = \frac{16}{Re}\frac{P}{A} \quad [9]$$

where Re, the modified Reynolds number, is defined by [A1.4].

4.2.1 *The conditions for zero relative velocity.* It is assumed that there is no interfacial shear at zero slip, which is a good approximation for turbulent–turbulent stratified flow, where the velocity profiles are relatively flat. The assumption is more questionable in the case of the laminar–turbulent stratified flow, but the real processes are more complicated than the simple stratified situation of the model and it is not considered warrented to use more detailed assumptions which would involve greater mathematical elaboration.

At zero slip the velocities of both phases are identical and equal to V and hence [8] simplifies to

$$1 = F\left(\frac{P}{A} - \frac{f_H \rho_H}{f_L \rho_L} \frac{1-P}{1-A}\right) \qquad [10]$$

where F, the modified Froude number, is defined as

$$F = \frac{f_L \rho_L V^2}{gR\Delta\rho \sin\alpha}. \qquad [11]$$

Equation [10] readily allows F to be calculated when the light phase is turbulent and f_L is constant. When the light phase flow is laminar, the following relationship between f_L and F can be established by application of [A1.3] and [11]

$$f_L = \frac{1}{F} \frac{64 \nu_L^2 \rho_L}{g\Delta\rho R^3 \sin\alpha} \left(\frac{P}{A}\right)^2. \qquad [12]$$

Substituting [12] into [10], we finally get

$$p^* \left(\frac{A}{P}\right)^2 \frac{1-P}{1-A} F^2 - \frac{P}{A} F + 1 = 0 \qquad [13]$$

where

$$p^* = \frac{\Delta p \rho_H f_H g R^3 \sin\alpha}{64 \nu_L^2 \rho_L^2}. \qquad [14]$$

The only admissible solution of [13] is

$$F = \frac{\frac{P}{A} - \sqrt{\left(\frac{P}{A}\right)^2 - 4\left(\frac{A}{P}\right)^2 \frac{1-P}{1-A} p^*}}{2\left(\frac{A}{P}\right)^2 \frac{1-P}{1-A} p^*}. \qquad [15]$$

Experimental data are compared with theoretical predictions in figure 10. In order to make the calculations, the following identities were necessary.

$$s = \sin\theta/\theta, \qquad [16]$$

$$P = \theta/\pi, \qquad [17]$$

$$A = \theta/\pi - \sin 2\theta/2\pi \qquad [18]$$

where θ is half-included angle for the ribbon.

The agreement between theory and experiment shown in figure 10 is reasonable considering the complex system that the mathematical model is representing.

4.2.2 *Slope of the relative velocity curve near zero slip.* We introduce the dimensionless slip velocity

$$W = \frac{V_L - V_H}{V_{HS}} \qquad [19]$$

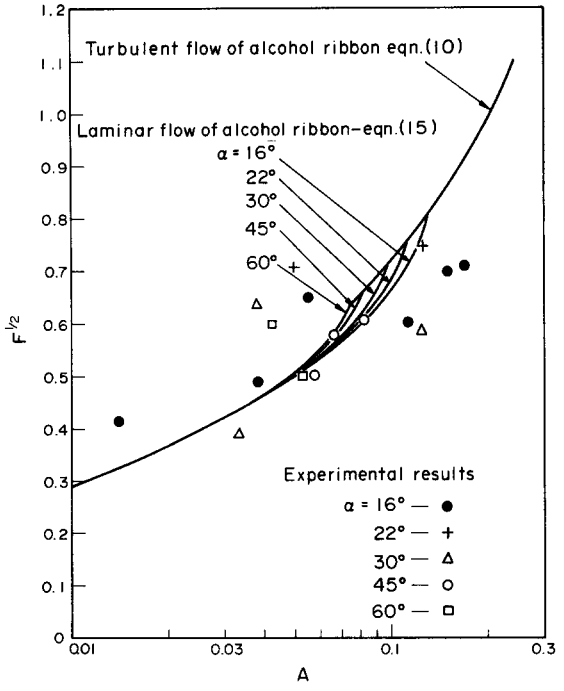

Figure 10. A plot of the square root of the modified Froude number, F, at zero slip vs the fractional area, A. Comparison of experimental results with theoretical predictions.

where V_{HS}, the superficial velocity of the heavy phase, is given by

$$V_{HS} = V_H(1-A). \qquad [20]$$

The slope of the slip velocity curve dW/dA, will be investigated on lines of constant V_{HS} in the vicinity of zero slip ($W = 0$).

For the turbulent flow of the light phase, it is assumed that, in addition to f_L and f_H being constant,

$$\tau_i = c_T W^2 \qquad [21]$$

where c_T is a constant independent of the alcohol fractional area, A.

Substituting [19] to [21] into [8] and differentiating with respect to A in the vicinity of $W = 0$ and with constant V_{HS}, we finally obtain:

$$\left[\frac{dW}{dA}\right]_{\substack{W=0 \\ V_{HS}=\text{const}}} = \frac{A(1-A)}{2P}\left\{\frac{3(1-P)-\dfrac{dP}{dA}(1-A)}{\dfrac{f_L\rho_L}{f_H\rho_H}(1-A)^4}+\frac{P(1-3A)-A(1-A)\dfrac{dP}{dA}}{A^2(1-A)^3}\right\} \qquad [22]$$

where dP/dA is given by

$$\frac{dP}{dA} = \frac{1}{1-\cos 2\theta}. \qquad [23]$$

For the laminar flow of the light phase, the wall friction factor, f_L, is given by [9] and it is further assumed that

$$\tau_i = c_L W \qquad [24]$$

where c_L is a constant independent of the fractional area, A.

Equations [9] and [24] are substituted into [8], which is then differentiated with respect to A in the vicinity of $W = 0$ and with constant V_{HS} to obtain

$$\left[\frac{dW}{dA}\right]_{\substack{W=0 \\ V_{HS}=\text{const}}} = \frac{\dfrac{A^2}{P^2}\left\{\dfrac{3(1-P)-(dP/dA)(1-A)}{\delta(1-A)^4}+\dfrac{P^2(2-3A)-2PA(1-A)(dP/dA)}{A^3(1-A)^2}\right\}}{1+\eta} \qquad [25]$$

where

$$\delta = \frac{8\nu_L\rho_L}{RV_S f_H \rho_H} \qquad [26]$$

$$\eta = \frac{s}{1-A}\frac{\tau_i/\Delta V}{(\tau_W)_L/V_L} \qquad [27]$$

and where ΔV, the relative velocity, is defined by [A2.6].

The function η must be determined for a complete solution to the problem. It is shown in appendix 2 the η can be approximated by

$$\eta = \frac{\pi}{4}\frac{sA}{1-A}\frac{1}{\psi} \qquad [28]$$

where

$$\psi = \frac{P}{A}(2/3\sin^3\theta - \pi A\cos\theta). \qquad [29]$$

if it can be assumed that the change in the slip for a change in the alcohol flowrate is dominated by and substantially equal to the change in the average alcohol velocity.

Substituting [28] and [29] into [25], we obtain the slope of the slip versus alcohol fractional area curve in the vicinity of zero slip for laminar flow of the light phase.

Experimental results are compared with the theory for both laminar and turbulent flow of the light phase in figure 11. Agreement is good.

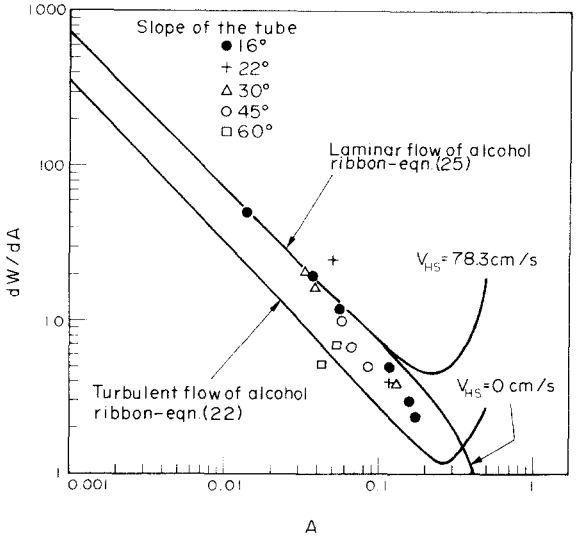

Figure 11. Plot of the slope of the relative velocity at zero slip, dW/dA, vs the fractional area A. Comparison of experimental data with theoretical predictions.

5. DISCUSSION

The success of the theoretical treatments suggests that there should be some confidence in extrapolating the condition for the break-up of a ribbon into drops by using the Weber number of [2] and in extrapolating the condition of ribbon flow by using the modified Froude number of [11]. However, some qualification of the last statement is required. Figure 12 shows $F^{1/2}$ plotted vs the alcohol fractional area A for various systems and for the condition that slip is zero. The alcohol–water system appears reasonably comparable to high pressure steam–water systems. Figure 13 on the other hand shows the more usual Froude number

$$F_V^{1/2} = \frac{V}{(gR \sin \alpha)^{1/2}} \qquad [30]$$

plotted vs A. The alcohol–water system does not appear such a good analogue of the steam–water system, chiefly because the alcohol flow is laminar. Geometrical similarity, which implies the same value of A in both analogue and prototype, can only be obtained with small flowrates in the analogue. It is seen, however, that the situation may be much improved by using, say, n-butyl acetate as the light phase. The comparison can be made even better by using a larger bore tube in the analogue to that in the prototype, for then the break between the turbulent and laminar curves will move to the left and the velocities in the systems will approach more closely to each other.

Lastly it is worth stressing the reason why air and water provides such a poor representation of low quality high pressure steam and water. It is noticed in figure 12, which is for the condition of zero relative velocity, that A has a maximum value, even if F is infinite. The condition for the maximum value of A is obtained by setting the bracketed term in [10] equal to zero. It is found by curve fitting results calculated from this condition, that the maximum value of $A = A_m$ is quite accurately given by

$$A_m = 0.5\left(\frac{f_L \rho_L}{f_H \rho_H}\right)^{1.54}. \qquad [31]$$

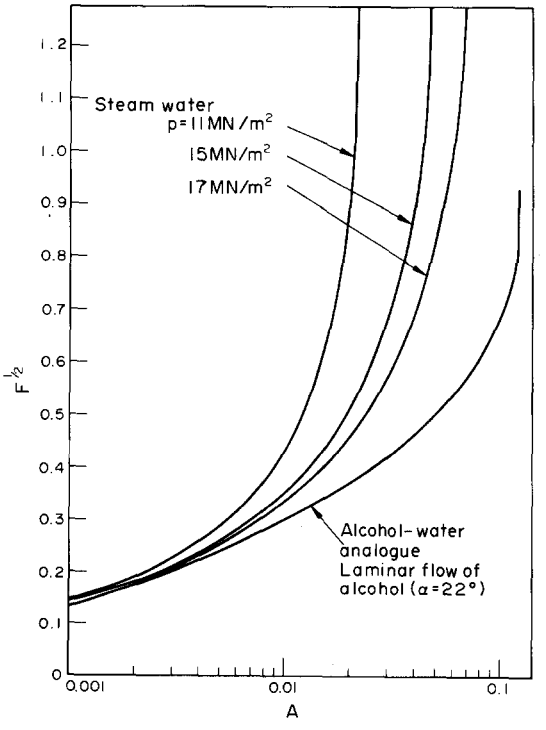

Figure 12. A plot of the square root of the modified Froude number, F, at zero slip vs the fractional area, A. Extension to high pressure steam–water systems.

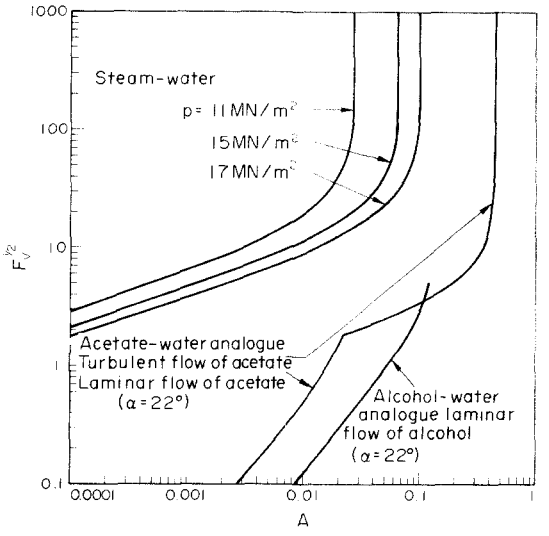

Figure 13. A plot of the square root of the Froude number, F_V, at zero slip vs the fractional area, A. Comparison of the alcohol–water analogue and butyl acetate–water analogue with high pressure steam–water systems.

We can deduce that A_m for steam and water at 11, 15 and 17 MN/m^2 is 0.027 ($2\theta = 59°$), 0.062 ($2\theta = 79°$) and 0.1 ($2\theta = 94°$). For air and water at atmospheric pressure $A_m = 2 \times 10^{-5}$ and $2\theta = 5°$. Clearly, if a stable ribbon is related to a condition of zero relative velocity, it will not be readily encountered in air–water systems.

Acknowledgement—This work was carried out at the Central Electricity Research Laboratories and is published by permission of the Central Electricity Generating Board.

REFERENCES

CHOJNOWSKI, B., WILSON, P. W. & WHITCUTT, R. D. B. 1974 Critical heat flux for inclined steam generating tubes, I. *Chem. Engrs Symp. Series* No. 38, *Paper* E3, *Symposium on Multiphase Flow Systems.*

GARDNER, G. C. & CROW, I. G. 1973 Onset of entrainment with a jet directed at a two-phase interface. *Chem. Engng Jl* **5**, 267–273.

GARDNER, G. C. & ADEBIYI, G. A. 1974 The liquid film left behind by a large bubble in a sloping channel. *Chem. Engng Sci.* **29**, 461–473.

HINZE, J. O. 1959 *Turbulence.* McGraw-Hill, New York.

RUSSELL, T. W. F., HODGSON, G. W. & GOVIER, G. W. 1959 Horizontal pipeline flow of mixtures of oil and water. *Can. J. Chem. Engng* **37**, 9–17.

STRAUB, L. G., SILBERMAN, E. & NELSON, H. C. 1956 Open channel flow at small Reynolds numbers. *J. Engng. Mech. Division. A.S.C.E. Proc.* **82**, Paper No. 1031.

APPENDIX 1

Calculation of the friction factor for the laminar flow

We will seek to demonstrate that a friction factor for laminar flow based upon the equivalent diameter concept is satisfactory for the purpose at hand. This concept states that

$$f_L = \frac{16}{\frac{V_L D_e}{\nu_L}} \qquad [A1.1]$$

where

$$D_e = \frac{4A_L}{P_L} \qquad [A1.2]$$

and using [5], [6], [17], [18], we obtain

$$f_L = \frac{16}{Re}\phi(\theta) \qquad [A1.3]$$

where

$$Re = \frac{2RV_L}{\nu_L} \qquad [A1.4]$$

$$\phi(\theta) = \frac{1}{1 - \dfrac{\sin 2\theta}{2\theta}}. \qquad [A1.5]$$

If the light phase occupies half of the cross section, $\theta = 90°$, $\phi(\theta) = 1$ and [A1.3] is identical with the solution for a liquid flowing through a semicircular channel with no shear stress at the free surface (Straub *et al.* 1956). Therefore, [A1.1] holds in the vicinity of $A = 0.5$.

Let us next investigate the friction factor for $\theta \to 0$. The Navier–Stokes equations, for the present case simplify to

$$\frac{dp}{dz} = \mu_L\left(\frac{\partial^2 v}{\partial x^2} + \frac{\partial^2 v}{\partial y^2}\right) \qquad [A1.6]$$

subject to

$$y = 0; \quad \frac{\partial v}{\partial y} = 0 \qquad [A1.7]$$

$$y = h; \quad v = 0 \qquad [A1.8]$$

where z is parallel to the tube axis, x is tangent to and y is normal to the crown of the cross-section. h is the depth of the alcohol at any point x, [A1.8] is the condition of zero slip at the tube wall and [A1.7] assumes that we are interested in zero shear at the water–alcohol interface because we are interested in the condition of zero slip.

It can be shown that

$$O\left(\frac{\partial^2 v}{\partial x^2}\right) \Big/ O\left(\frac{\partial^2 v}{\partial y^2}\right) = \tan^2\frac{\theta}{2} \qquad [A1.9]$$

where $O(a)$ means order of magnitude of quantity a. Hence for small θ, [A1.6] simplifies to

$$\frac{dp}{dz} = \mu_L \frac{d^2 v}{dy^2} \qquad [A1.10]$$

whose solution, subject to [A1.7] and [A1.8], is

$$v = \frac{1}{2\mu_L}\frac{dp}{dz}[y^2 - h^2]. \qquad [A1.11]$$

Also, from the force equilibrium (pressure drop is equal to the frictional drop)

$$\frac{A_L}{P_L}\frac{dp}{dz} = \frac{1}{2} f_L \rho_L V_L^2 \qquad [A1.12]$$

where V_L is the mean velocity of the light phase defined by

$$V_L = \frac{1}{A_L}\int_{A_L} v \, dA_L \qquad [A1.13]$$

we finally obtain,

$$f_L = \frac{16}{Re}\zeta(\theta) \qquad [A1.14]$$

where

$$\zeta(\theta) = \frac{3}{2}\left(\frac{A}{P}\right)^2 \frac{1}{\frac{A}{P}(2\cos^2\theta + 13) - 10\sin^2\theta}. \qquad [A1.15]$$

Equation [A1.14] becomes exact as $\theta \to 0$.

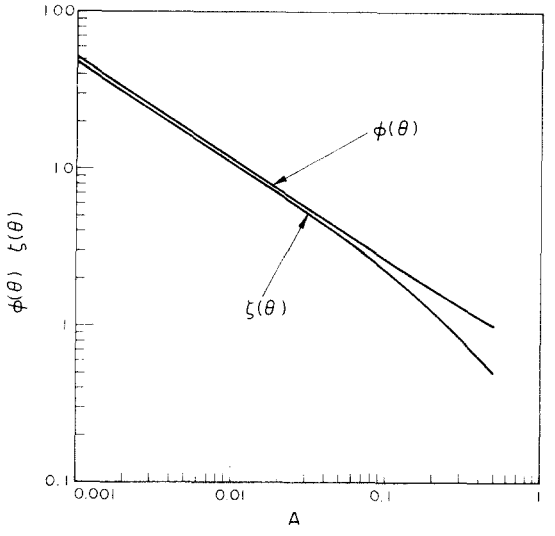

Figure 14. Comparison of functions $\Psi(\theta)$ and $\zeta(\theta)$.

Functions $\phi(\theta)$ and $\zeta(\theta)$ are compared in figure 14. Since for small θ they are nearly identical (as $\theta \to 0$, $\phi(\theta) \to 36/24\theta^2$ and $\zeta(\theta) \to 35/24\theta^2$), [A1.3] is reasonably accurate for small A as well near $A = 0.5$ and is therefore employed in the body of this paper. It is also helpful to note that

$$\phi(\theta) = \frac{P}{A}. \qquad [A1.16]$$

APPENDIX 2

Calculation of function η

To simplify the calculations it will be assumed that θ is small and that [A1.10] applies. With zero interfacial shear, the mean velocity of the light phase, V_L is given in appendix 1 and can be calculated to be

$$V_L = -\frac{2}{3\mu_L}\frac{dp}{dz}R^2\frac{\omega(\theta)}{\pi A} \qquad [A2.1]$$

where

$$\omega(\theta) = \frac{\pi}{8}\{A(2\cos^2\theta + 13) - 10P\sin^2\theta\}. \qquad [A2.2]$$

If a constant interfacial shear, τ_i is introduced, [A1.10] and [A1.8] remain unchanged and [A1.7] modifies to

$$y = 0; \quad \frac{dv}{dy} = \frac{\tau_i}{\mu_L}. \qquad [A2.3]$$

The local velocity is then given as

$$v' = \frac{1}{2\mu_L}\frac{dp}{dx}(y^2 - h^2) + \frac{\tau_i}{\mu_L}(y - h) \qquad [A2.4]$$

and the mean velocity, V_L', as

$$V_L' = -\frac{1}{\pi A}\left\{\frac{2}{3\mu_L}\frac{dp}{dz}R^2\omega(\theta) + \frac{\tau_i}{\mu_L}R\frac{A}{P}\psi(\theta)\right\} \qquad [A2.5]$$

where $\psi(\theta)$ is given by [29].

The relative velocity, ΔV, subject to assumptious of Section 4.2.2, is defined as

$$\Delta V = V_L' - V_L \qquad [A2.6]$$

and can thus be calculated from [A2.1] and [A2.5] as

$$\Delta V = \frac{\tau_i}{\mu_L}\frac{R}{\pi P}\psi. \qquad [A2.7]$$

Thus

$$\frac{\tau_i}{\Delta V} = \frac{\pi P \mu_L}{R\psi} \qquad [A2.8]$$

and since

$$T_{wL} = \frac{1}{2}\rho_L f_L V_L^2 \qquad [A2.9]$$

where f_L is given by [9.9] we finally obtain

$$\eta = \frac{\pi}{4}\frac{sA}{1-A}\frac{1}{\psi}. \qquad [A2.10]$$